Application Note

Life Science Research

Agilent

Trusted Answers

# Restoring Mitochondrial Function to Drive Neuroblastoma Differentiation

## Using complementary metabolic analyses with an Agilent Seahorse XF analyzer, an Agilent 6545 LC/Q-TOF, and an Agilent BioTek Cytation 5 cell imaging multimode reader


**Authors**

Haowen Jiang, Sarah Jane Tiche, Clifford JiaJun He, Junyan Liu, Fuyun Bian, Mohamed Jedoui, Balint Forgo, Md Tauhidul Islam, Pamela Emengo, Bo He, Yang Li, Albert M. Li, Meng-Ning Zhou, Katrin J. Svensson, Florette K. Hazard, Lei Xing, Hiroyuki Shimada, Bill Chiu, and Jiangbin Ye
Stanford University
Stanford, CA, USA

Meng Zhao
University of California Davis
Davis, CA, USA

Anh T. Truong, Jestine Ho, Cate Simmermaker, Yanan Yang, and Daniel J. Cuthbertson
Agilent Technologies, Inc.
Santa Clara, CA, USA



## Abstract

Mitochondrial dysfunction is a hallmark of cancer and contributes to dedifferentiation and tumor progression. In this study, researchers used a combination of retinoic acid (RA) and a mitochondrial uncoupler (NEN) to restore mitochondrial quantity and quality in neuroblastoma cells. The Agilent Seahorse XF analyzer revealed enhanced mitochondrial respiration, while the Agilent 6545 LC/Q-TOF confirmed a metabolic shift from glycolysis to oxidative phosphorylation. Additionally, the Agilent BioTek Cytation 5 cell imaging multimode reader enabled visualization of mitochondrial morphology, providing phenotypic evidence of differentiation. Together, these platforms delivered a comprehensive view of mitochondrial reprogramming and its role in promoting tumor cell differentiation. This work highlights the power of integrating functional, molecular, and imaging-based tools for metabolism measurement in cancer research.

## Introduction

Neuroblastoma is a pediatric solid tumor arising from neural crest cells, and it accounts for approximately 15% of childhood cancer-related deaths. The prognosis of neuroblastoma is strongly linked to the degree of tumor cell differentiation—more differentiated tumors are associated with improved survival outcomes.[1,2] One of the key features of aggressive neuroblastoma is a metabolic shift known as the Warburg effect, in which cells rely on aerobic glycolysis rather than mitochondrial oxidative phosphorylation, even in the presence of oxygen.[3] This shift is driven by mitochondrial dysfunction and is associated with dedifferentiation, increased proliferation, and resistance to therapy.[4,5]

Retinoic acid (RA), a derivative of vitamin A, is an agent used to promote differentiation in neuroblastoma and leukemia. RA increases mitochondrial biogenesis by upregulating nuclear-encoded mitochondrial genes and boosting mitochondrial DNA (mtDNA) copy number.[6] However, RA alone does not activate mitochondrial respiration or reverse the Warburg phenotype. This is likely due to insufficient ATP turnover in dedifferentiated cells, which leads to a buildup of mitochondrial membrane potential and inhibition of the electron transport chain (ETC).[7]

To overcome this limitation, researchers combined RA with niclosamide ethanolamine (NEN), a mitochondrial uncoupler. NEN dissipates the mitochondrial membrane potential, thereby stimulating ETC activity, increasing $NAD^+$/NADH ratios, and promoting ATP turnover.[8] This combination therapy restores both mitochondrial quantity and quality, reactivates the tricarboxylic acid (TCA) cycle, and shifts metabolism from biosynthesis to energy production.[9]

In this study, researchers used a multiplatform approach to evaluate the effects of RA and NEN on neuroblastoma metabolism and differentiation:

- The Seahorse XF Pro analyzer was used to measure real-time mitochondrial respiration, including basal and maximal oxygen consumption rates (OCR), spare respiratory capacity, and energy phenotype.
- The 6545 LC/Q-TOF enabled $^{13}$C-glucose and $^{13}$C-glutamine isotope tracing to quantify metabolic flux through glycolysis, the pentose phosphate pathway, and the TCA cycle.
- The Cytation 5 cell imaging multimode reader provided high-content imaging to visualize mitochondrial morphology and neurite outgrowth, a phenotypic marker of neuronal differentiation.

Together, these platforms revealed that RA+NEN treatment synergistically increased mitochondrial count, restored mitochondrial function, elevated $NAD^+$/NADH ratios, and reactivated the TCA cycle (Figure 1). These changes were accompanied by a reversal of dedifferentiation and the emergence of neuron-like morphology, highlighting the therapeutic potential of targeting mitochondrial metabolism in neuroblastoma.

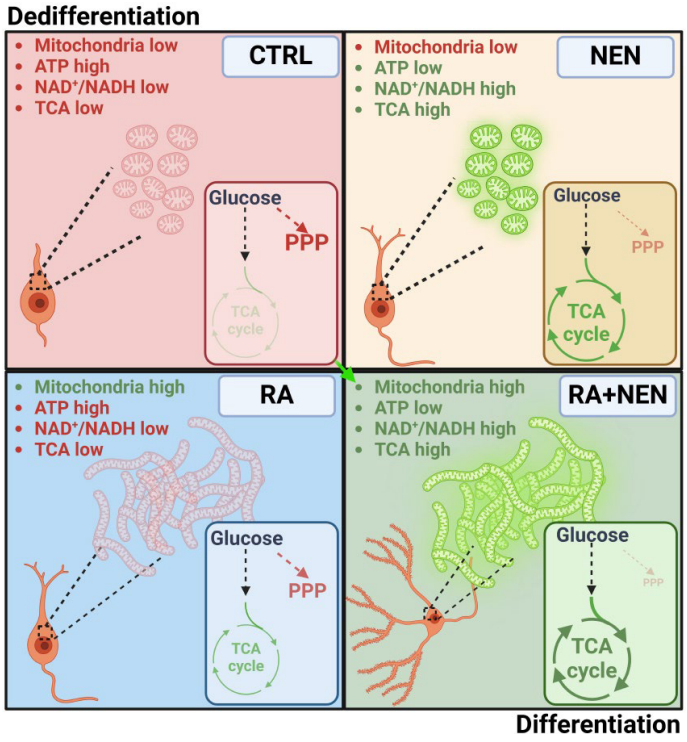


**Figure 1.** Effect of combined retinoic acid and niclosamide ethanolamine therapy on neuroblastoma metabolism and differentiation.

## Experimental

### Mitochondrial respiration assay

Neuroblastoma cell lines SK-N-BE(2) and CHP134 were seeded in Seahorse XFe96/XF Pro cell culture microplates (part number 103794-100) and treated with 1 µM RA, 1 µM NEN, a combination of both, or dimethyl sulfoxide (DMSO) control for 72 hours. Mitochondrial respiration was assessed using the Seahorse XF Pro analyzer and the Seahorse XF Cell Mito Stress Test kit (part number 103015-100). The assay measured basal respiration, ATP production-coupled respiration, maximal respiration, and spare respiratory capacity. Cell number normalization was performed using Hoechst 33342 staining and quantified with the Cytation 5 cell imaging multimode reader.

### LC/MS-based metabolomics and isotope tracing

To assess metabolic flux, cells were treated with RA, NEN, or both for 72 hours, followed by a 5-hour incubation with either U-$^{13}C_6$-glucose or U-$^{13}C_5$-glutamine. Metabolites were extracted using chilled methanol and water, filtered using Agilent Captiva EMR–Lipid cartridges, and dried prior to analysis.

Targeted metabolomics and isotope tracing were performed using an Agilent 1290 Infinity II LC coupled to a 6545 LC/Q-TOF, following the standardized workflow outlined in Yannell *et al.*[10] Chromatographic separation was achieved using an Agilent InfinityLab Poroshell 120 HILIC-Z column. Data acquisition and analysis were conducted using Agilent MassHunter Profinder and Quantitative Analysis software. A custom personal compound database and library (PCDL) built from METLIN was used to identify and quantify glycolytic and TCA cycle intermediates. Isotopologue distributions were corrected for natural abundance and normalized to total protein content.

### Imaging and mitochondrial morphology analysis

To visualize mitochondrial morphology and assess differentiation, cells were transduced with a 3xHA-OMP25-GFP construct to fluorescently label mitochondria. Cells were seeded in 96-well plates using FluoroBrite DMEM to reduce background fluorescence. After treatment, mitochondrial content and morphology were monitored using the Cytation 5 cell imaging multimode reader, which provided environmental control and automated image acquisition. At endpoint, Hoechst 33342 was added to stain nuclei, and images were analyzed using Agilent BioTek Gen5 data analysis software.

## Results and discussion

This study demonstrates the power of integrating Seahorse XF Pro, 6545 LC/Q-TOF, and Cytation 5 imaging technologies to characterize the metabolic and phenotypic effects of restoring mitochondrial function in neuroblastoma cells. A full account of this study can be found in Jiang *et al.*[6]

### Seahorse XF analysis reveals functional mitochondrial recovery

Seahorse XF analysis showed that RA alone increased mitochondrial biogenesis, as evidenced by elevated spare and maximal respiratory capacity, but did not enhance basal respiration (Figure 2). NEN alone slightly increases basal respiration and spare capacity relative to control, suggesting modest mitochondrial improvement. RA + NEN shows comparable basal respiration but enhanced maximal and spare capacity, indicating better mitochondrial function.

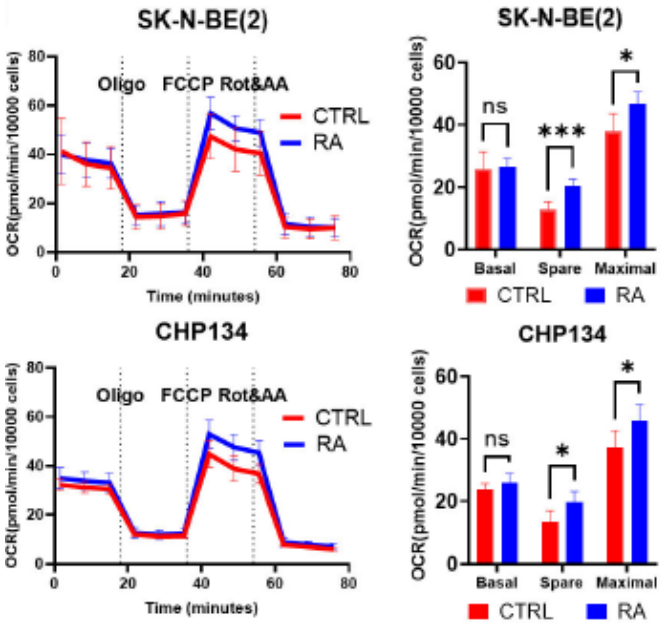


**Figure 2.** Retinoic acid increases mitochondrial content without enhancing respiration. Mitochondrial respiration was measured using an Agilent Seahorse XF analyzer, capturing basal, spare, and maximal oxygen consumption rates (OCR).

Energy phenotype mapping revealed that RA+NEN-treated cells shifted from a quiescent to an energetic state, indicating restored mitochondrial activity (Figure 3B). These findings confirm that mitochondrial uncoupling is necessary to activate respiration in RA-primed cells.

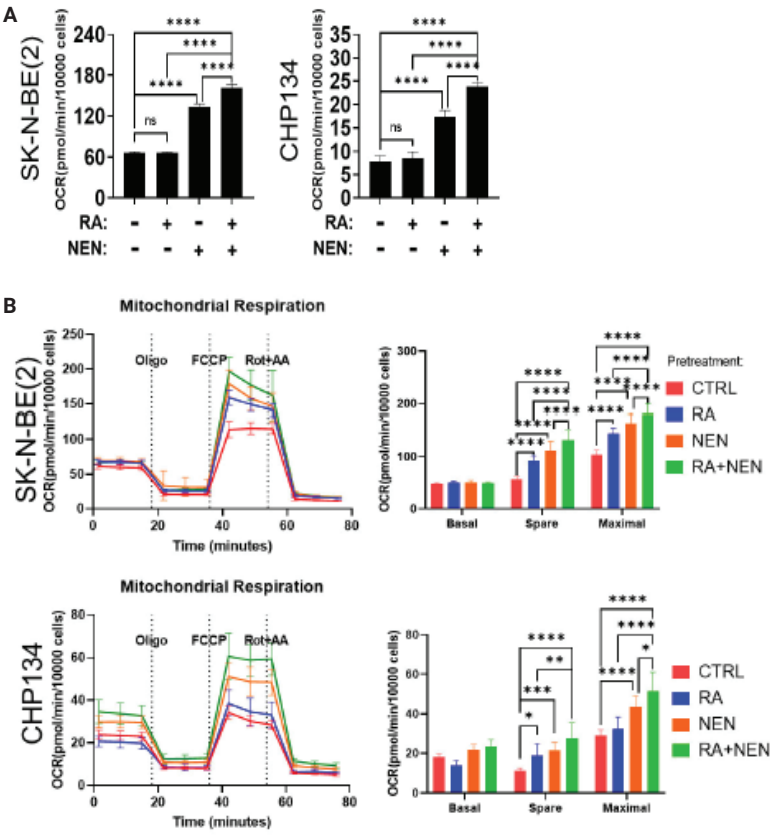


**Figure 3.** Retinoic acid and mitochondrial uncoupler (NEN) synergistically enhance respiration and shift metabolism toward oxidative pathways. (A) Basal oxygen consumption rates (OCR) were measured in SK-N-BE(2) and CHP134 cells after 72-hour treatment with RA, NEN, RA+NEN, or vehicle control using an Agilent Seahorse XF analyzer. (B) Seahorse XF analysis of basal respiration, spare capacity, and maximal respiratory capacity in cells pretreated with each condition.

### LC/MS-based metabolomics reveals metabolic reprogramming

LC/MS-based metabolomics analysis reinforced the Seahorse XF findings that RA increased mitochondrial biogenesis but did not activate mitochondrial respiration or shift metabolism toward oxidative phosphorylation (Figure 4). Additionally, the combination of RA and NEN restored mitochondrial function by creating a pseudo-ATP demand that activated respiration. This led to a lower ATP/ADP ratio and a higher $NAD^+$/NADH ratio, signaling enhanced ETC activity and oxidative metabolism (Figure 5A).

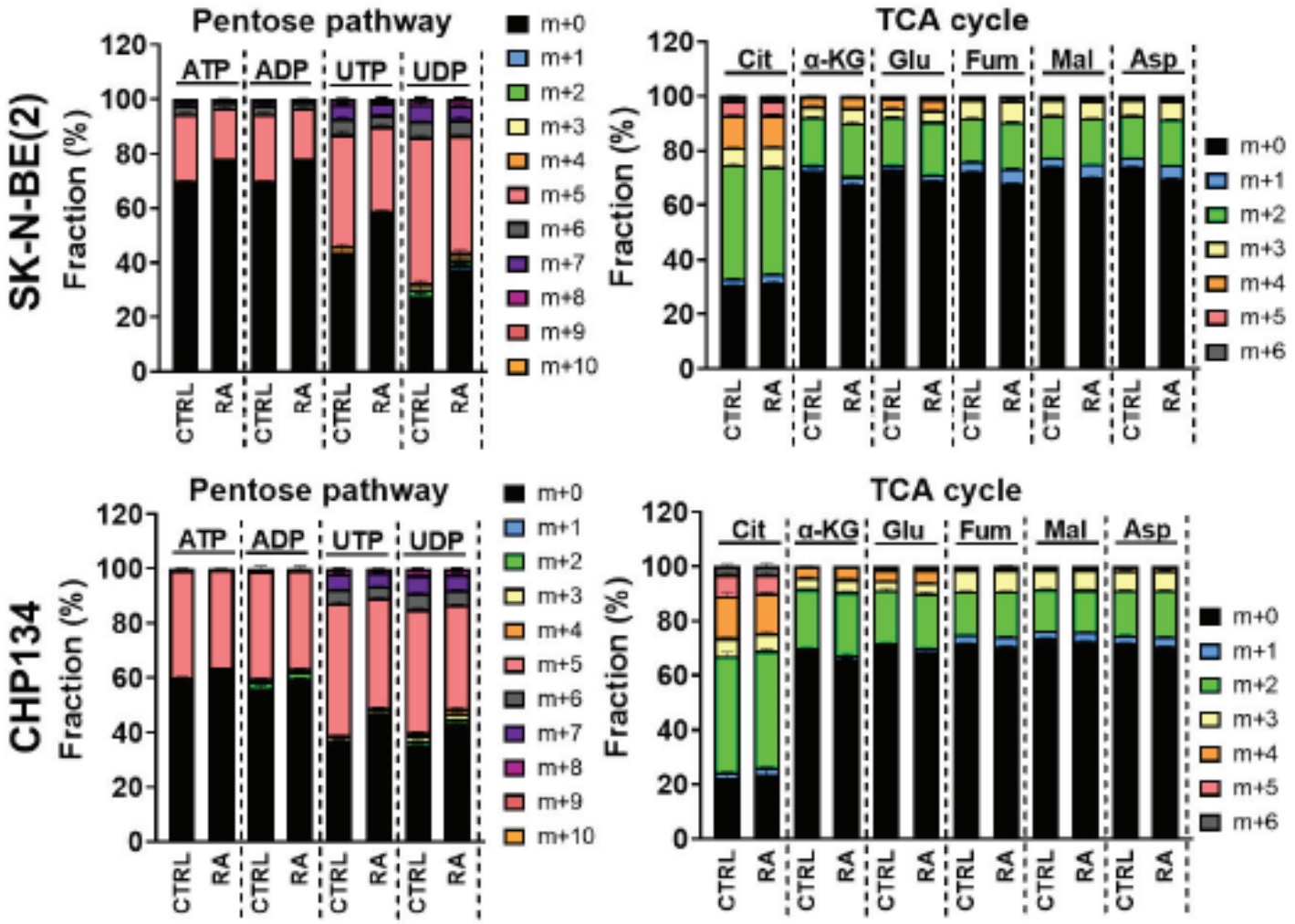


**Figure 4.** Retinoic acid increases mitochondrial content without enhancing respiration. LC/MS analysis of $^{13}C$-labeled glucose incorporation into metabolites of the pentose phosphate pathway and TCA cycle.

Stable isotope tracing with $^{13}$C-glucose and $^{13}$C-glutamine revealed that RA+NEN treatment reprogrammed cellular metabolism. LC/MS analysis showed a reduction in glucose carbon flux into the pentose phosphate pathway and nucleotide biosynthesis, and a redirection into the TCA cycle (Figure 5B). This was evidenced by increased labeling of TCA intermediates such as citrate, α-ketoglutarate, and malate.

Glutamine tracing further supported this shift, showing reduced reductive carboxylation and increased oxidative metabolism (Figure 5C). These changes were consistent with Seahorse data and confirmed that RA+NEN restored mitochondrial function and reversed the Warburg effect.

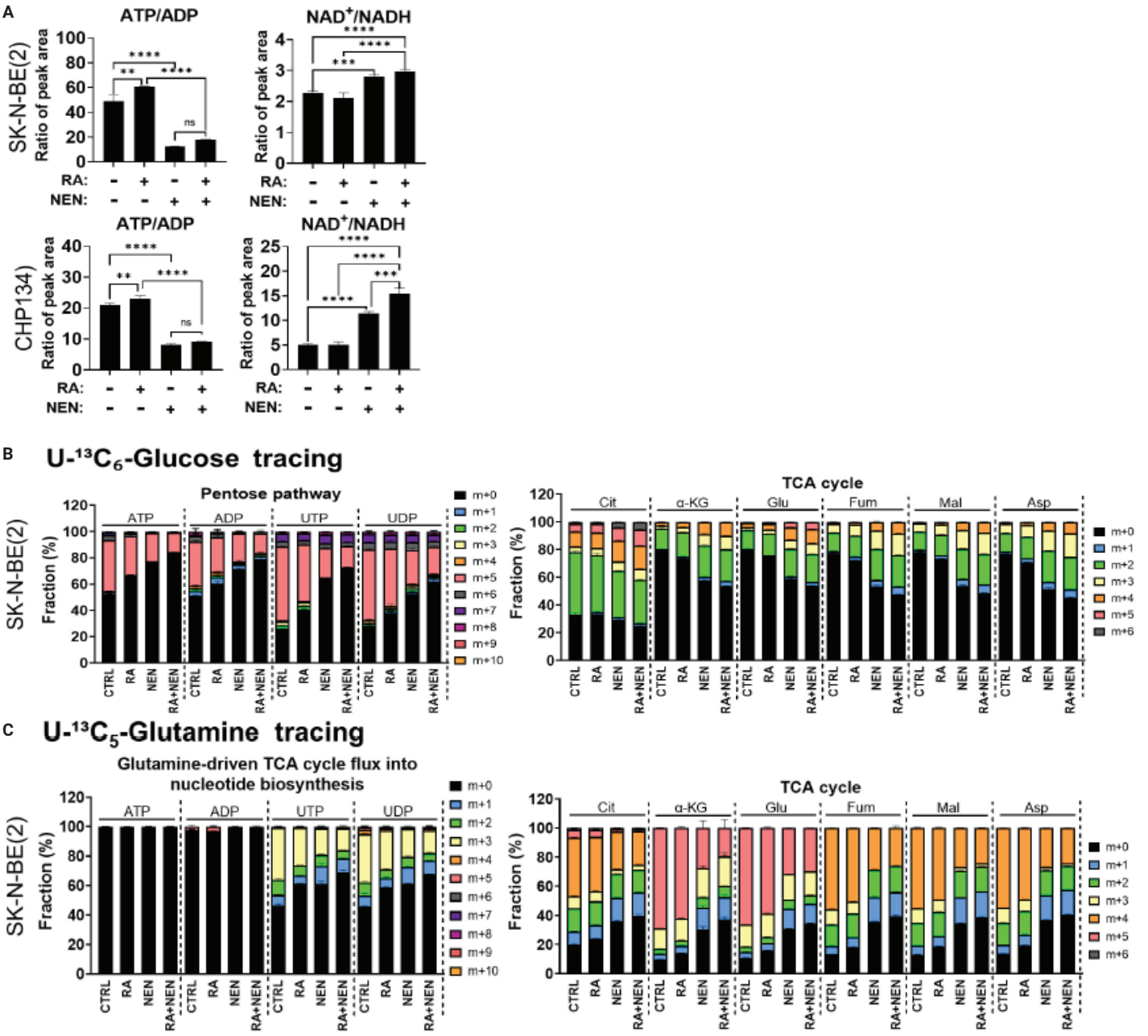


**Figure 5.** Retinoic acid and mitochondrial uncoupler (NEN) synergistically enhance respiration and shift metabolism toward oxidative pathways. (A) Intracellular ATP/ADP and NAD$^+$/NADH ratios were quantified by LC/MS to assess energy balance and redox state. (B,C) LC/MS-based $^{13}$C-glucose and $^{13}$C-glutamine tracing revealed treatment-dependent changes in carbon flux through the pentose phosphate pathway and TCA cycle.

## Cytation 5 imaging confirms mitochondrial remodeling and differentiation

The Cytation 5 was used to visualize mitochondrial biogenesis. Cells expressing the 3xHA-OMP25-GFP reporter showed increased mitochondrial mass and elongation following RA treatment (Figure 6). RA treatment also led to a significant increase in linear mitochondria, a hallmark of functional mitochondrial networks.

RA and NEN individually increased neurite number and length, but the combination produced a synergistic effect (Figure 7A). Immunofluorescence staining for β-Tubulin III confirmed the neuronal identity of differentiated cells (Figure 7B). These results demonstrate that mitochondrial remodeling is tightly linked to phenotypic differentiation.

## Integrated insights from Agilent platforms

Together, the Seahorse XF analyzer, 6545 LC/Q-TOF, and Cytation 5 cell imaging multimode reader provided a complete picture of how RA and NEN reprogram neuroblastoma metabolism. Seahorse measured mitochondrial function in real time, LC/MS revealed underlying metabolic shifts, and Cytation 5 linked these changes to visible cellular differentiation. This integrated approach enabled a deeper understanding of how mitochondrial restoration supports therapeutic differentiation in cancer.

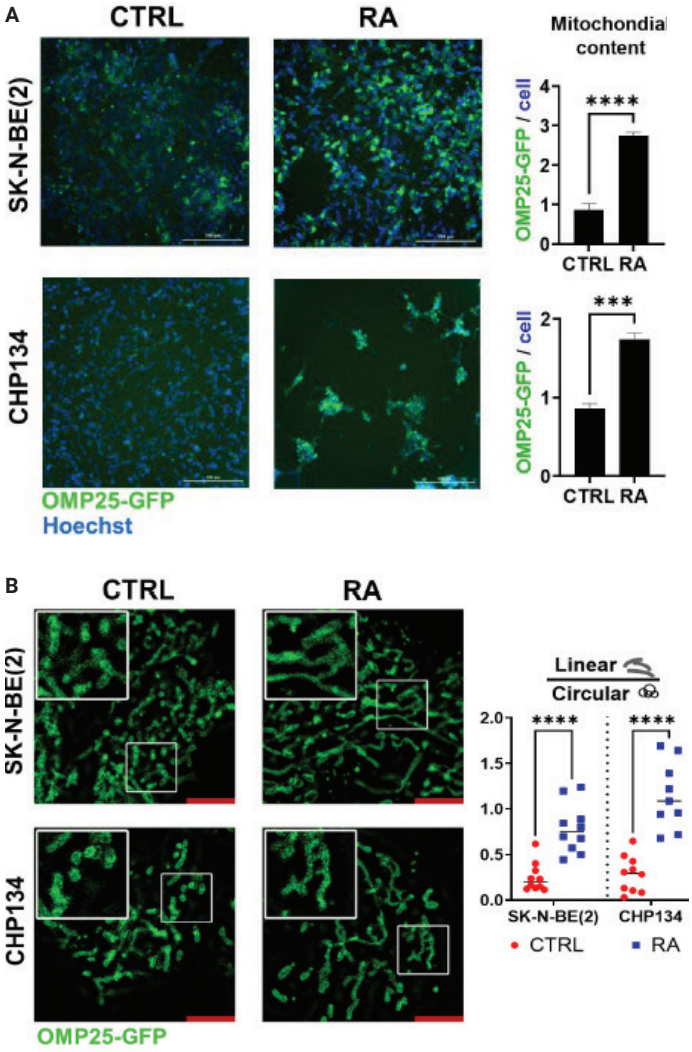


**Figure 6.** Retinoic acid increases mitochondrial content without enhancing respiration. (A) SK-N-BE(2) and CHP134 neuroblastoma cells expressing 3xHA-OMP25-GFP (green) were treated with 1 µM RA or DMSO (control) for 72 hours. Nuclei were stained with Hoechst (blue), and mitochondrial signal intensity was normalized to nuclear staining. (B) Confocal microscopy was used to evaluate mitochondrial morphology, with quantification of linear versus circular forms.

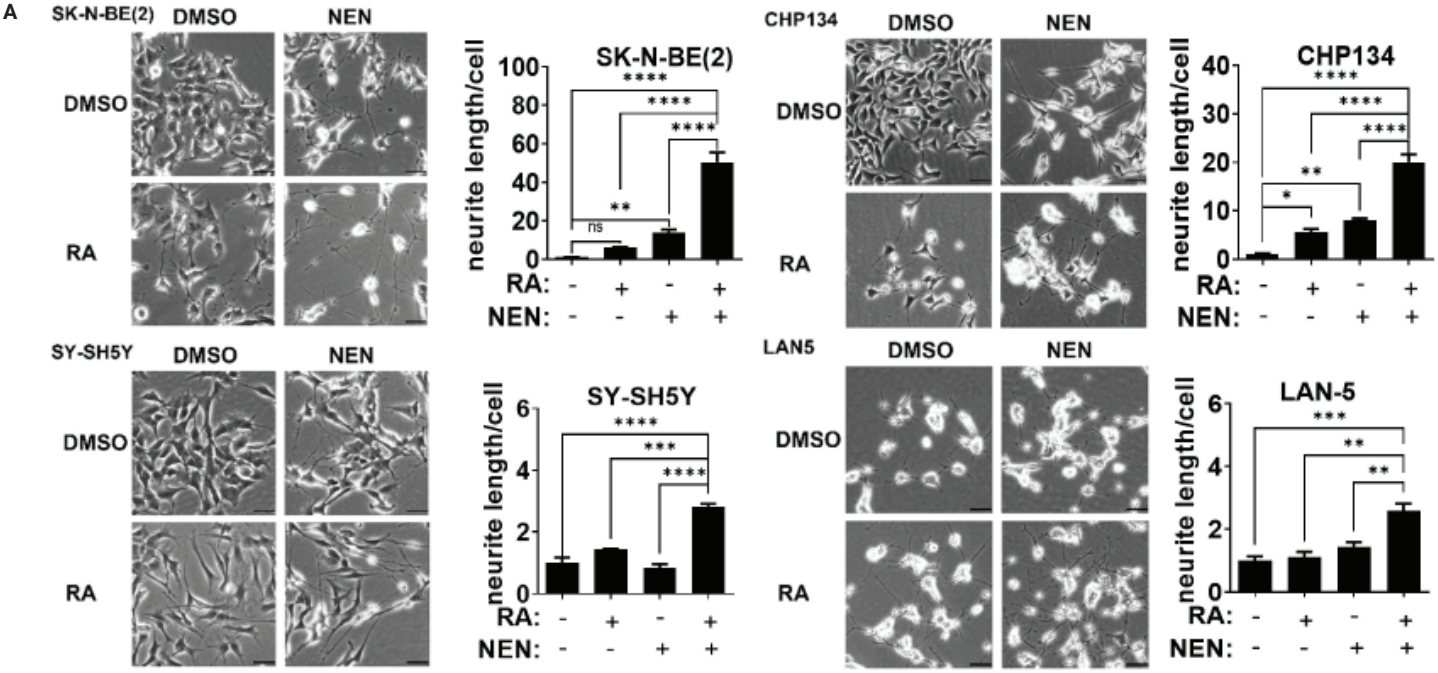


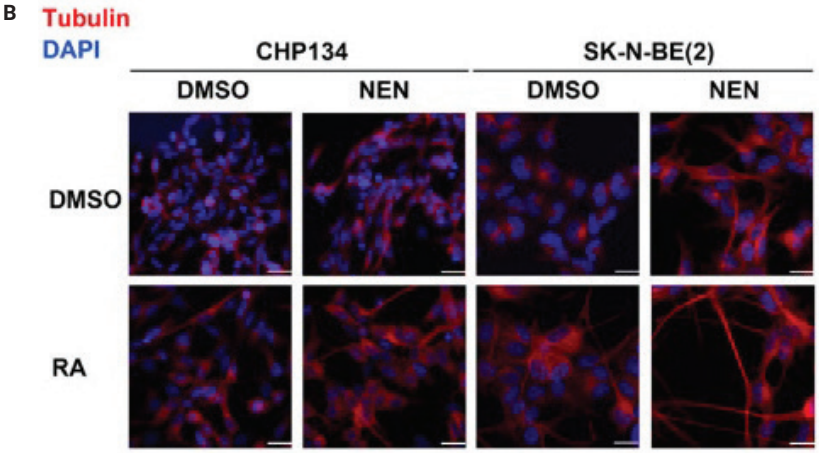


**Figure 7.** Retinoic acid and NEN synergistically promote neuronal differentiation in neuroblastoma cells. (A) Phase-contrast microscopy of SK-N-BE(2), CHP134, SH-SY5Y, and LAN-5 cells treated with DMSO (control), RA, NEN, or the RA+NEN combination. Neurite outgrowth was quantified by measuring average neurite length per cell. Scale bar: 25 µm. (B) Immunofluorescence staining of β-Tubulin III (red) and DAPI (blue) in SK-N-BE(2) and CHP134 cells highlights enhanced neurite formation following treatment.

## Conclusion

This study demonstrates the power of combining Agilent Seahorse XF, Agilent 6545 LC/Q-TOF, and Agilent BioTek Cytation 5 technologies to gain a comprehensive understanding of mitochondrial restoration and differentiation in neuroblastoma. Seahorse XF provided real-time functional insights into mitochondrial respiration, LC/MS revealed underlying shifts in metabolic flux, and Cytation 5 delivered high-content imaging of mitochondrial biogenesis and neuronal differentiation. Together, these platforms offered a multidimensional view of how metabolic reprogramming drives phenotypic change—insights that would not have been possible using any single technology alone.

## References


1. Maris, J. M.; Hogarty, M. D.; Bagatell, R.; Cohn, S. L. Neuroblastoma. *Lancet* **2007**, *369*, 2106–2120.
2. Matthay, K. K.; *et al.* Neuroblastoma. *Nat. Rev. Dis. Primers* **2016**, *2*, 16078.
3. Vander Heiden, M. G.; Cantley, L. C.; Thompson, C. B. Understanding the Warburg Effect: The Metabolic Requirements of Cell Proliferation. *Science* **2009**, *324*, 1029–1033.
4. DeBerardinis, R. J.; Chandel, N. S. We Need to Talk About the Warburg Effect. *Nat. Metab.* **2020**, *2*, 127–129.
5. Li, A. M.; Ye, J. Deciphering the Warburg Effect: Metabolic Reprogramming, Epigenetic Remodeling, and Cell Dedifferentiation. *Annu. Rev. Cancer Biol.* **2024**, *8*, 35–58.
6. Jiang, H.; *et al.* Restoring Mitochondrial Quantity and Quality to Reverse Warburg Effect and Drive Neuroblastoma Differentiation. *Proc. Natl. Acad. Sci. U.S.A.* **2025**, *122*, e240123456.
7. Zhao, Y.; *et al.* In Vivo Monitoring of Cellular Energy Metabolism Using SoNar, a Highly Responsive Sensor for $NAD^+$/NADH Redox State. *Nat. Protoc.* **2016**, *11*, 1345–1359.
8. Tao, H.; *et al.* Niclosamide Ethanolamine-Induced Mild Mitochondrial Uncoupling Improves Diabetic Symptoms in Mice. *Nat. Med.* **2014**, *20*, 1263–1269.
9. Jiang, H.; *et al.* Mitochondrial Uncoupling Induces Epigenome Remodeling and Promotes Differentiation in Neuroblastoma. *Cancer Res.* **2023**, *83*, 181–194.
10. Yannell, K.; Simmermaker, C.; Van de Bittner, G.; Cuthbertson, D. An End-to-End Targeted Metabolomics Workflow. *Agilent Technologies application note*, publication number 5994-5628EN, **2023**.


**www.agilent.com**


DE-012706





Printed in the USA, February 25, 2026
5994-8727EN


Agilent
Trusted Answers